A PHASE-CHANGE APPROACH TO MACRO-PARTICLE PYROLYSIS OF CELLULOSIC MATERIALS.

R. E. DEROSIERS and R. J. LIN

Chemical Engineering Department, Texas Tech University, Lubbock, TX 79409

INTRODUCTION

Biomass is a solid fuel with a high content (approx. 80%) of volatile matter (VM) as defined by standard proximate analyses. As a result, the devolatilization of the material introduced into any thermal conversion device is the most significant process occurring on a mass basis. From the viewpoint of reactor design, it would be convenient to have closed form expressions for the rate of pyrolysis of large particles of cellulosic materials suitable for the convective-heat-transfer environment of the packed or fluidized bed reactor.

The state of knowledge of the fundamental aspects of the pyrolysis "reaction" is advancing rapidly through kinetic studies on small, finely-divided samples in which physical transport considerations are minimized. The Arrhenius rate expressions resulting from these studies are reflective, it is hoped, of the intrinsic chemical reaction rates of pyrolysis processes. The high cost of comminution of feedstock to small mesh sizes however, dictates against the large scale conversion of biomass in this form. Thermal conversion of cellulosic materials in packed or fluidized beds will most likely be accomplished with particle sizes in the range of one to eight cm. With dimensions of that magnitude, the relative rates of chemical and transport processes must be considered.

An indication of the disparity in chemical versus heat transfer rates is afforded by the observation of "advancing front" behavior in the pyrolysis of cylindrical samples of biomass materials (Blackshear, Murty, 1966). The low thermal conductivity and high reactivity of biomass result in a narrow, advancing, reacting zone of pyrolysis. The sharply peaked reaction rate profile results from the depletion of VM in the char and a low temperature level in the virgin solid. The validity of this reaction rate profile is supported by experimental density and temperature profiles. If the reaction rate was slower,

the density profile would be less sharply stepped. The acceleration of the heat transfer rate in the virgin solid would likewise result in a more gradual transition.

Several pyrolysis models have been proposed (Bamford (1946), Roberts (1963), Blackshear (1966), Maa (1973), Lee (1982)) in order to faithfully reproduce the detailed pyrolysis behavior of large samples of cellulosic materials. These usually involve the solution of coupled partial differential equations (PDE's) representing mass, energy, and momentum balances. These models may be classified into two general categories. Volumetric models (Fan, 1978) are the most sophisticated and complex. The rate of decomposition is calculated at the local temperature throughout the solid. Shrinking core models (Maa, 1973) take the advancing front behavior to the limit of an infinitesimally thin reaction zone. In the former case, the reaction is a source term in the conservation equations while in the latter case, the reaction rate appears as a boundary condition. The continuing effort to describe ever more accurately the complicated phenomena of pyrolysis will doubtless give rise to more complex models.

The complexity of the single-particle model used to describe the pyrolysis process will be augmented however, when this model is integrated into the simulation of a gasification reactor. Thus it is our goal to move in the direction of simpler, albeit less precise, models of macro-particle pyrolysis. Consider the computational burden involved in the simulation of a packed-bed reactor. The conservation equations for the bed require an iterative solution because of split boundary conditions. (For example, solid temperature at one terminus, and gas temperature at the other.) For each iteration of the equations for the bed, many evaluations of the reaction rate for the particle must be made. If the evaluation of this rate at each point requires a finite-difference solution of a set of coupled PDE's for the particle, then the calculation time becomes excessive.

The model considered below may be called kinetics-free in that no explicit consideration is given to the rate of pyrolysis. The controlling influence on the rate of decomposition is the heat transfer rate. The progress of the pyrolysis is followed by the rate of advance of a sharp boundary defined as the locus of points at a fixed pyrolysis temperature, T_p. The resulting model is similar in many respects to a phase change problem. In fact, the process may be considered as a change in phase from one solid form (wood) to another (char).

We have been investigating the suitability of such a model in decribing the pyrolysis of 0.5 to 2.5 cm cylindrical samples of natural and densified wood. The objectives of the work are:

1. Develop the proper forms of the relevant equations of change; select an appropriate set of dimensionless variables.
2. Develop efficient numerical schemes to integrate the coupled partial-differential equations and to generate temperature profiles and rate vs time curves.
3. Determine if the model can even crudely reproduce experimental temperature profiles and pyrolysis times without extensive curve fitting. That is, by selecting realistic values of physical parameters, can an a priori calculation produce feasible results.
4. Perform a sensitivity analysis to determine which parameters have the greatest influence on the rate of advance of the pyrolysis front.
5. Determine to what extent the model is capable of faithfully reproducing the details of pyrolysis phenomena even if some parameters must be curve-fitted.

THE PHENOMENA OF PYROLYSIS

Before considering the development of the phase-change model of pyrolysis, it is worthwhile to list some of the more important processes occurring in pyrolysis in order to assess their relevance to any simulation.

Reaction: The primary events of pyrolysis are being intensively studied and it is clear that considering pyrolysis as a single reaction with a fixed product slate is a gross oversimplification. The classification of species as primary and secondary products is far from complete. The expertise to predict in detail even the overall ("final") products of the process is not available. It is not even possible to predict in advance for any feed the precise char yield under different heating rates. It is therefore entirely reasonable to represent pyrolysis crudely as

$$\text{wood} = c\ \text{char} + b\ \text{volatiles}$$

Heat of Reaction: Thermodynamic arguments indicate quite clearly that the overall pyrolysis process is exothermic. TGA studies support this contention. There is some doubt however concerning the amount of char produced by primary and secondary events. The exothermicity is directly proportional to char production. It could be possible for example to have an endothermic primary reaction producing some char and mostly reduced gases such as CO, followed by an exothermic conversion to CO_2 and more carbon at a different location. Since the heat of pyrolysis depends on the spectrum of products, and the spectrum of products depends strongly on the conditions imposed to cause pyrolysis, it is not unreasonable to assume that the primary decomposition is endothermic. Indeed, when carried out under inert atmospheres, some differential scanning calorimetry studies have indicated that this is the case (Muhlenkamp (1975)).

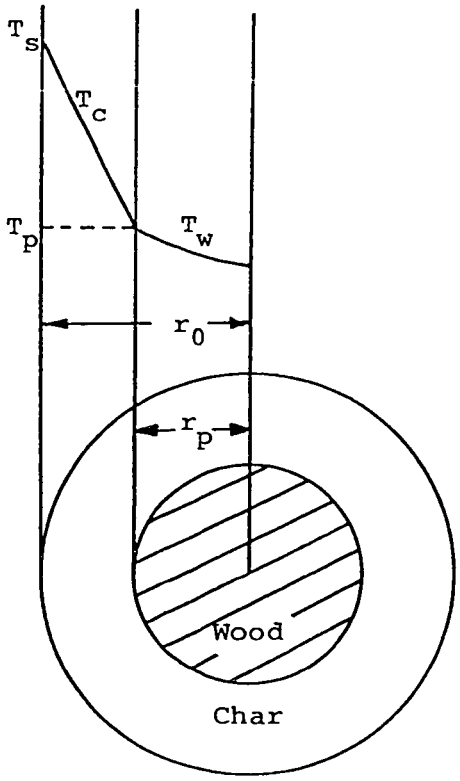

Figure 1: Pyrolysis Scheme of a Single Particle Under the Boundary Condition of First Kind

Reaction Rate: The possibility of representing the rate of decomposition of a mixture of linear polysaccharides and a cross-linked phenylpropane polymer with a single Arrhenius rate expression appears remote. At best it seems likely that a distribution of activation energies would be required. It is assumed below that the rate of decomposition is fast relative to the rate of heat transfer necessary to sustain the pyrolysis.

Geometry: Some shrinkage does occur during pyrolysis as evidenced by checking and pitting of char layers. But this effect will be ignored and constant diameter assumed. Of more importance is the porosity of chars and the resulting effects on density and resistance to gas flow. In this work, the porosity is assumed sufficiently great that the hydrodynamics of gas flow can be ignored. A cylindrical particle geometry has been used in this study.

Gas Flow: A unidirectional, outward flow of non-condensible gases must occur during pyrolysis. But condensible species such as water may be forced inward and result in a net flow towards the cooler, inner region of the cylinder. Water condensing in the layers immediately adjacent to the pyrolysis zone has been proposed by some investigators to explain the delay in the development of the inner temperature profile of samples of pressed cellulose. This inward flow of condensibles has not as yet been considered in the development of the phase-change model but could crudely be accommodated by using a higher effective heat capacity for the unpyrolyzed solid. A better approximation could be made by considering two "phase" changes: in effect, a drying wave and a pyrolysis wave passing through the sample.

THE PHASE CHANGE MODEL OF PYROLYSIS

The simulation of pyrolysis proposed here seeks to avoid the mathematical complexity of the volumetric model as well as the pre-selection of the pyrolysis rate inherent in the steady-state, moving-boundary approach. Maa (1973), for example, uses a kinetic expression for the rate of pyrolysis, but fixes the temperature at which it is evaluated, resulting in a steady state. The pseudo steady-state is probably a reasonable assumption for a large piece of wood (a log or beam) but is probably not valid for a one-cm particle.

To proceed, we make the following assumptions:

1. The pyrolysis reaction may be considered simply as:

   $$\text{Feed} = b\ \text{Gas} + c\ \text{Char}$$

   Here "Gas" refers to all volatile products, and "char" to the completely devolatilized solid. The reaction occurs instantaneously when the solid is raised to a fixed temperature, T_p.
2. Heat is conducted through the char layer to a surface separating char and unpyrolyzed solid. This surface is defined as the locus of points at $T = T_p$. At this surface, the temperature is continuous, but a jump occurs in the temperature gradient, the magnitude of which is determined by the heat of pyrolysis and the thermal properties of the two solids.
3. The temperature of escaping volatiles is always equal to the local char temperature, T_c.

Although not necessary, the following assumptions have been made for convenience in this initial development:

4. Thermal properties (heat capacity, conductivity) and density are assumed constant at an effective or average value.
5. Cylindrical geometry.
6. Specified surface temperature (B.C. of 1st kind).

The mathematical formulation of the model is derived from the equation of change for energy. In the char layer

$$\frac{\partial}{\partial t}(\rho_c c_{pc} T_c) + \frac{\partial}{\partial \underline{r}} \cdot (-k_c \frac{\partial T}{\partial \underline{r}} + \rho_g c_{pg} T_c \underline{u}_g) = 0$$

The third term is the convective flux of gas. A mass balance at any radial location yields an expression for the gas flux.

$$\rho_g u_g = - b \rho_w \frac{r_p}{r} \frac{dr_p}{dt}$$

where r_p is the location of the advancing front. Ordinary conduction occurs in the fresh solid region. (Hereafter referred to as wood.) The system of equations to be solved in each region in cylindrical geometry are

$$\frac{\partial T_c}{\partial t} = \alpha_c \left(\frac{\partial^2 T_c}{\partial r^2} + \frac{1}{r} \frac{\partial T_c}{\partial r} \right) + b \frac{\rho_w}{\rho_c} \frac{c_{pg}}{c_{pc}} \frac{r_p}{r} \frac{dr_p}{dt} \frac{\partial T_c}{\partial r}$$

$$r_p < r < r_o \qquad t > 0$$

With no gas flux in the core:

$$\frac{\partial T_w}{\partial t} = \alpha_w \left(\frac{\partial^2 T_w}{\partial r^2} + \frac{\partial T_w}{r \partial r} \right) \qquad 0 < r < r_p \qquad t > 0$$

$$\text{IC:}\quad T_w = T_i \qquad 0 < r < r_o \qquad t = 0$$

$$\text{BC: (1)}\quad T_c = T_s \qquad r = r_o \qquad t > 0$$

$$\text{(2)}\quad T_c = T_w = T_p \qquad r = r_p \qquad t > 0$$

$$\text{(3)}\quad k_w \frac{\partial T_w}{\partial r} - k_c \frac{\partial T_c}{\partial r} = \rho_w (\Delta H) \frac{dr_p}{dt} \qquad r = r_p \qquad t > 0$$

$$\text{(4)}\quad \frac{\partial T_w}{\partial r} = 0 \qquad r = 0 \qquad t > 0$$

The system of equations is non-linear because of the convective term as well as the third boundary condition (Carslaw, Jaeger, 1959). It is of the same form as a simple phase change problem, with the exception of the convective term. Exact solutions on infinite domains are available (Stefan, 1891; Ockendon and Hodgkins, 1975). Comparable problems on finite geometries are usually solved numerically. Extensive bibliographies are available (Selim, Roberts, 1981; Wilson, et. al., 1978). The numerical procedure developed by Roberts (1981) is used here. This procedure is facilitated by the introduction of the following dimensionless parameters:

$$R = 1 - r/r_o \qquad \tau = \alpha_c \, t/r_o^2$$

$$U = \left(\frac{k_c}{k_w}\right) \frac{T_c - T_p}{T_p - T_i} \qquad V = \frac{T_w - T_p}{T_p - T_i}$$

$$T_s^* = \frac{k_c}{k_w} \frac{T_s - T_p}{T_p - T_i} \qquad T_i^* = \frac{T_i - T_p}{T_p - T_i} = -1$$

$$\alpha^* = \alpha_c / \alpha_w \qquad \Delta H^* = \frac{\alpha_c}{\alpha_w} \frac{\Delta H}{C_{pw}(T_p - T_i)}$$

$$B = 1 + b \frac{\rho_w}{\rho_c} \frac{C_{pg}}{C_{pc}} (R_p - 1) \frac{dR_p}{d\tau}$$

The dimensionless form of the system of equations is

$$\frac{\partial U}{\partial \tau} = \frac{\partial^2 U}{\partial R^2} + \frac{B}{R - 1} \frac{\partial U}{\partial R} \qquad 0 < R < R_p \quad \tau > 0 \qquad (1)$$

$$\frac{\partial V}{\partial \tau} = \frac{1}{\alpha^*} \frac{\partial^2 V}{\partial R^2} + \frac{1}{R - 1} \frac{\partial V}{\partial R} \qquad R_p < R < 1 \quad \tau > 0 \qquad (2)$$

IC $V = -1$ $\qquad 0 < R < 1 \quad \tau = 0 \qquad (3)$

BC $U = T_s^*$ $\qquad R = 0 \quad \tau > 0 \qquad (4)$

$U = V = 0$ $\qquad R = R_p \quad \tau > 0 \qquad (5)$

$$\frac{dR_p}{d\tau} = \left(\frac{\partial V}{\partial R} - \frac{\partial U}{\partial R} \right) \frac{1}{\Delta H^*} \qquad R = R_p \quad \tau > 0 \qquad (6)$$

$$\frac{\partial V}{\partial R} = 0 \qquad R = 1 \quad \tau > 0 \qquad (7)$$

Finite Difference Formulation

The finite difference form of the numerical algorithm requires a finite, non-zero value of R_p. If a fixed surface temperature is imposed with $T_s > T_p$, then the Stefan analytical solution is used to obtain a starting position of the pyrolysis front. A standard explicit finite difference scheme is used to advance through the first time step and a Dufort Frankel scheme (which requires

temperatures at a previous time) is used for all subsequent time steps. If a time dependent surface temperature, beginning with $T_s < T_p$ is imposed, then the numerical integration of the straight-forward conduction problem with no pyrolysis front is implemented until the temperature at a finite value of R reaches T_p, at which time the Dufort Frankel scheme with a moving boundary is begun. Temperatures at points adjacent to either terminus R = 0 or R = 1, or the moving boundary are calculated with the usual approximations. The details are presented below.

In order to approximate the solution of the parabolic partial differential equations, (1) and (2), a network of grid points with equal size in the R-direction and equal size in the time step is established throughout the region $0 < R < 1$, $0 < \tau$.

A DuFort-Frankel scheme (Carnahan, 1969) was chosen to obtain a finite difference solution to the parabolic partial differential equations. Adequate accuracy was obtained with 21 grid points and $\Delta t/(\Delta R)^2 < 0.5$.

The DuFort-Frankel Scheme requires data from two previous time levels. The standard explicit scheme is used as a starting method to provide the required data. Eqs. (1) and (2) expressed in the standard explicit scheme (see Figure 2) are given by

$$\frac{U_{i,j+1} - U_{i,j}}{\Delta\tau} = \frac{U_{i-1,j} - 2U_{i,j} + U_{i+1,j}}{(\Delta R)^2} + \frac{B}{(i\Delta R - 1)} \frac{(U_{i+1,j} - U_{i-1,j})}{2\Delta R} \qquad i = 1,2,\ldots,M-1 \qquad (8)$$

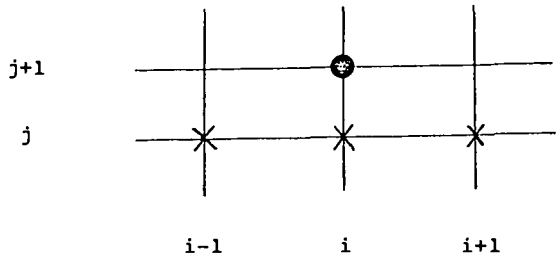

Standard Explicit Scheme

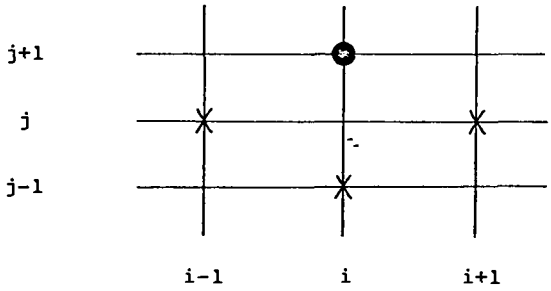

DuFort-Frankel Scheme

Figure 2: Graphic Description of Finite-Difference Scheme.

$$\frac{V_{i,j+1} - V_{i,j}}{\Delta\tau} = \frac{1}{\alpha^*}\frac{V_{i-1,j} - 2V_{i,j} + V_{i+1,j}}{(\Delta R)^2} + \frac{1}{(i\Delta R - 1)}\frac{(V_{i+1,j} - V_{i-1,j})}{2\Delta R} \qquad i = M+2, M+3, \ldots, N-1 \qquad (9)$$

and M indicates the nearest grid point to the left of the pyrolyzing front (see Figure 3). These two equations are rearranged and solved for the unknown terms $U_{i,j+1}$ and $V_{i,j+1}$ to give:

$$U_{i,j+1} = (1 - 2\lambda)U_{i,j} + \lambda\left[\left(1 - \frac{B}{2(i - \frac{1}{R})}\right)U_{i-1,j} + \left(1 + \frac{B}{2(i - \frac{1}{R})}\right)U_{i+1,j}\right] \qquad i = 1,2,\ldots,M-1 \qquad (10)$$

$$V_{i,j+1} = \left(1 - \frac{2\lambda}{\alpha^*}\right)V_{i,j} + \frac{\lambda}{\alpha^*}\left[\left(1 - \frac{1}{2(i - \frac{1}{\Delta R})}\right)V_{i-1,j} + \left(1 + \frac{1}{2(i - \frac{1}{\Delta R})}\right)V_{i+1,j}\right] \qquad i = M+2, M+3, \ldots, N-1 \qquad (11)$$

where $\lambda = \Delta\tau/(\Delta R)^2$.

Expressed in the DuFort-Frankel Scheme, Equations (1), (2) become

$$\frac{U_{i,j+1} - U_{i,j-1}}{2\,\Delta\tau} = \frac{U_{i-1,j} - U_{i,j+1} - U_{i,j-1} + U_{i+1,j}}{(\Delta R)^2} + \frac{B}{(i\Delta R - 1)}\frac{(U_{i+1,j} - U_{i-1,j})}{2\Delta R} \qquad i = 1,2,\ldots,M-1 \qquad (12)$$

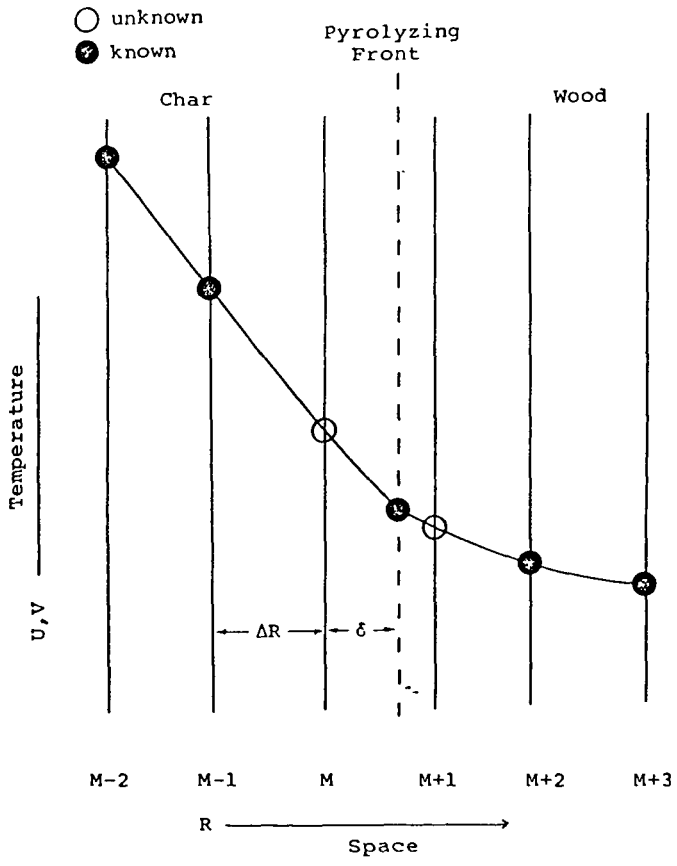

Figure 3: 3-Point Lagrangian Interpolation for the unknow temperature U_M, V_{M+1} Adjacent to the pyrolysis front.

$$\frac{V_{i,j+1} - V_{i,j-1}}{2\Delta\tau} = \frac{1}{\alpha^*} \frac{V_{i-1,j} - V_{i,j+1} - V_{i,j-1} + V_{i+1,j}}{(\Delta R)^2} +$$

$$\frac{1}{(i\Delta R - 1)} \frac{(V_{i+1,j} - V_{i-1,j})}{2\Delta R} \qquad i = M+1, M+2, \ldots, N \qquad (13)$$

Equations (12) and (13) are rearranged and solved for the unknown terms $U_{i,j+1}$, $V_{i,j+1}$ to give

$$U_{i,j+1} = \frac{1 - 2\lambda}{1 + 2\lambda} U_{i,j-1} + \frac{2\lambda}{1 + 2\lambda} \left[\left(1 - \frac{B}{2(i - \frac{1}{\Delta R})}\right) U_{i-1,j} + \left(1 + \frac{1}{2(i - \frac{1}{\Delta R})}\right) U_{i+1,j} \right] \qquad i = 1,2,\ldots,M-1 \qquad (14)$$

$$V_{i,j+1} = \frac{1 - \frac{2\lambda}{\alpha^*}}{1 + \frac{2\lambda}{\alpha^*}} V_{i,j-1} + \frac{\frac{2\lambda}{\alpha^*}}{1 + \frac{2\lambda}{\alpha^*}} \left[\left(1 - \frac{1}{2(i - \frac{1}{\Delta R})}\right) V_{i-1,j} + \left(1 + \frac{1}{2(i - \frac{1}{\Delta R})}\right) V_{i+1,j} \right] \qquad i = M+1, M+2, \ldots, N \qquad (15)$$

The singularity of Equation (2) at R = 1 is prevented by using L'Hopital's rule to yield

$$\frac{\partial V}{\partial \tau} = -\frac{2}{\alpha^*} \frac{\partial^2 V}{\partial R^2} \qquad R = 1 \quad \tau > 0 \qquad (16)$$

This equation written in the standard explicit form is given by

$$\frac{V_{i,j+1} - V_{i,j}}{\Delta\tau} = \frac{2}{\alpha^*} \frac{(V_{i-1,j} - 2V_{i,j} + V_{i+1,j})}{(\Delta R)^2} \qquad (17)$$

and in the Dufort-Frankel Scheme by

$$\frac{V_{i,j+1} - V_{i,j-1}}{2\Delta T} = -\frac{2}{\alpha^*} \frac{(V_{i-1,j} - V_{i,j+1} - V_{i,j-1} + V_{i+1,j})}{(\Delta R)^2} \qquad i = N \qquad (18)$$

Equation (7) can be written in finite-difference form using a central difference approximation to give

$$\frac{V_{N+1,j} - V_{N-1,j}}{2\Delta R} = 0.$$

Combined with Equation (18) this yields an expression for the center-line dimensionless temperature

$$V_{N,j+1} = (1 - \frac{4\lambda}{\alpha^*})V_{N,j} + \frac{4\lambda}{\alpha^*} V_{N-1,j} \qquad R = 1 \qquad (19)$$

in the standard explicit form and

$$V_{N,j+1} = \frac{1 - \frac{4\lambda}{\alpha^*}}{1 + \frac{4\lambda}{\alpha^*}} V_{N,j-1} \quad \frac{\frac{8\lambda}{\alpha^*}}{1 + \frac{4\lambda}{\alpha^*}} V_{N-1,j} \qquad R = 1 \qquad (20)$$

in the DuFort-Frankel Scheme.

Grid Points M, M+1

The temperatures at grid points immediately adjacent to the pyrolyzing front (grid points M and M+1 in Figure 3) cannot be calculated by Equations (10)-(11) and (14)-(15). Instead, a three-point Lagrangian interpolation is used to determine these unknown temperatures.

$$U_{M,j} = \frac{-\delta}{(2\Delta R + \delta)} U_{M-2,j} + \frac{2\delta}{(\Delta R + \delta)} U_{M-1,j} \qquad i = M \qquad (21)$$

$$V_{M+1,j} = \frac{2(\Delta R - \delta)}{(2\Delta R - \delta)} V_{M+2,j} + \frac{(\Delta R - \delta)}{(3\Delta R + \delta)} V_{M+3,j} \qquad i = M+1 \tag{22}$$

Where

$$\delta = R_p - R_M = R_p - M\Delta R$$

Grid Points M = 1,2

When the pyrolyzing front is located within the first grid space, Equation (21) is not required, since the boundary value $U_{0,j}$ is already known.

If the pyrolyzing front is located within the second grid space, Equation (21) cannot be used because the required three points are not available. By assuming that the temperature profile within the char layer is quadratic in R, the derivatives U/τ, U/R, $^2U/R^2$ in equation (1) can be approximated to yield.

$$\frac{U_{2,t+1} - U_{2,t}}{\Delta\tau} = \frac{2}{\Delta R(\Delta R + \delta)} U_{1,t} - \frac{2}{\Delta R(\delta)} U_{2,t+1} - \left(\frac{B}{\Delta R - 1}\right)\left(\frac{\delta}{\Delta R(\Delta R + \delta)}\right)U_{1,t}$$

$$- \left(\frac{\Delta R - \delta}{\Delta R(\delta)}\right)U_{2,t+1} \tag{23}$$

which can be solved for $U_{2,t+1}$

Advancing the Pyrolysis Front

Euler's method (Carnahan, 1969) is used to solve the energy balance across the pyrolyzing surface, Eq. 9. The march of the pyrolysis front is computed from the following finite difference form of Eq. 9.

$$R_p\Big|_{\tau=\tau+\Delta\tau} - R_p\Big|_{\tau} = \Delta R_p = \frac{\Delta\tau}{\Delta H^*}\left(\frac{\partial U}{\partial R} - \frac{\partial V}{\partial R}\right)\Bigg|_{R=R_p},$$

The temperature gradients are approximated by differentiation of the three-point Lagrangian interpolation formulas, Equations (21) and (22), to give

$$\left(\frac{\partial U}{\partial R}\right)_{R=R_p} = \frac{(\Delta R + \delta)}{(2\Delta R + \delta)\Delta R} U_{M-2,j} - \frac{(2\Delta R + \delta)}{(\Delta R + \delta)\Delta R} U_{M-1,j} \tag{24}$$

$$\left(\frac{\partial V}{\partial R}\right)_{R=R_p} = \frac{(3\Delta R - \delta)}{(2\Delta R - \delta)\Delta R} U_{M+2,j} - \frac{(2\Delta R - \delta)}{(3\Delta R - \delta)\Delta R} U_{M+3,j} \tag{25}$$

When the pyrolyzing front is within the first grid space, two point interpolation formulas are used to approximate the temperature gradient in the char layer.

$$\left(\frac{\partial U}{\partial R}\right)_{R=R_p} = -\frac{U_{1,j}}{R_p} \tag{26}$$

When the pyrolyzing front is located within the second grid space, a quadratic polynomial is used to approximate the temperature gradient in the char layer. The gradient at the pyrolyzing front is

$$\left(\frac{\partial U}{\partial R}\right)_{R=R_p} = \frac{-\delta}{\Delta R(\Delta R + \delta)} U_{1,j} - \frac{\Delta R + \delta}{\Delta R(\delta)} U_{2,j} \tag{27}$$

Since the temperature of the unreacted core is so close to the pyrolysis temperature when the pyrolyzing front moves into the last two grid spaces, a two point interpolation formula is used to approximate the temperature gradient in the wood layer. The temperature of the unreacted core is taken equal to the pyrolysis temperature and the temperature gradient in the wood layer at $R = R_p$ becomes equal to zero thereafter.

Since the advance of the front during the last time step may place it beyond R = 1, a three point Lagrangian interpolation formula is used to find the time required for complete the pyrolysis.

$$\tau_p = \frac{(1 - R_{p2})(1 - R_{p3})}{(R_{p1} - R_{p2})(R_{p1} - R_{p3})}\tau_1 + \frac{(1 - R_{p1})(1 - R_{p3})}{(R_{p2} - R_{p1})(R_{p2} - R_{p3})}\tau_2 + \frac{(1 - R_{p1})(1 - R_{p2})}{(R_{p3} - R_{p1})(R_{p3} - R_{p2})}\tau_3$$

Where R_{p1}, R_{p2}, R_{p3} = the last three computed R_p values.

τ_1, τ_2, τ_3 = the three times corresponding to the above values.

SENSITIVITY STUDY

Using the numerical procedures described above, temperature profiles at various times were generated. Sample profiles are illustrated in figure 4. The time required for the pyrolysis front to reach the centerline of the cylinder was defined as t_{pyr}.

The effect of each model parameter on the time required for complete pyrolysis was studied in order to determine its relative importance. A base case was constructed by selecting average values for the parameters (as listed in Table 1) and calculating the pyrolysis time. Values of t_{pyr} were then determined for several cases in which each parameter was varied individually. Sensitivity was defined as $\Delta t_{pyr}/\Delta p$, where Δp is the change in the value of the parameter studied from its base value. A negative sensitivity indicates increasing p will decrease t_{pyr}.

The results of the sensitivity study are summarized in Table 2 and illustrated in Figure 5.

Temperature Profile

With Convection Term.

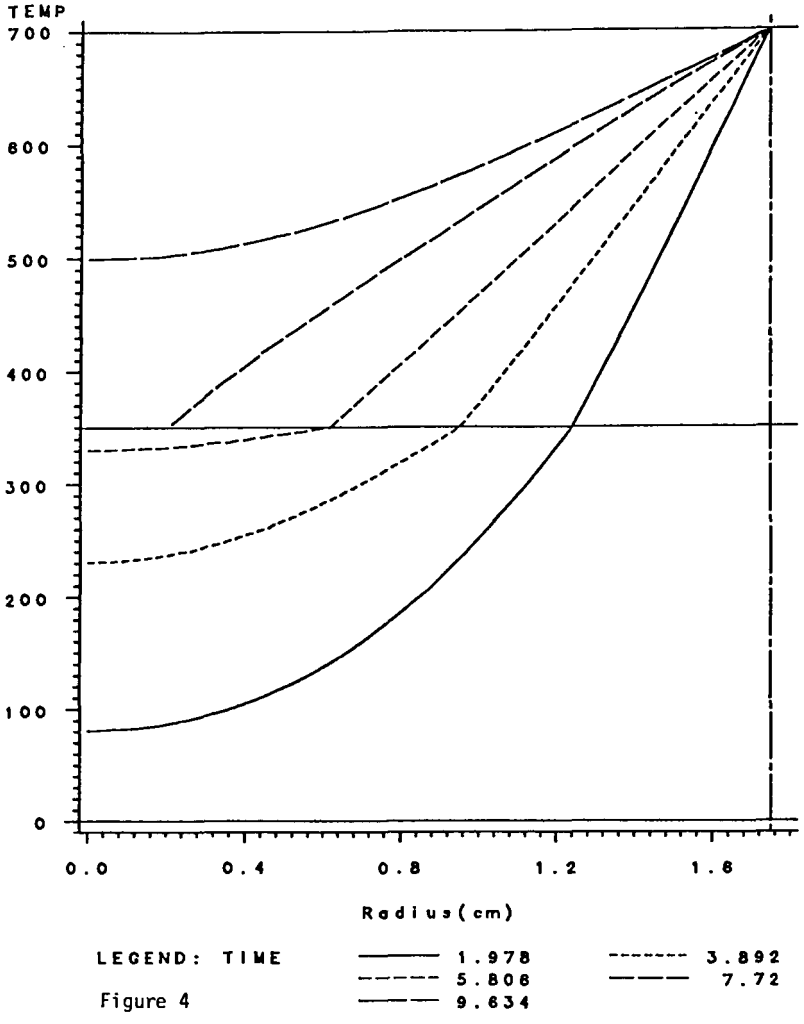

Figure 4

Table 1

Typical Values of Model Parameters Used in Sensitivity Study

ρ_w =	1230.0	Kg/M^3
ρ_c =	$\rho_w(1-b)$	
C_{pw} =	1318.0	Joule/Kg
C_{pc} =	991.6	Joule/Kg
k_w =	0.2000	Joule/M-Sec-K
k_c =	0.20	Joule/M-Sec-K
r_o =	0.01	m
T_s =	700.0	C
T_p =	350.0	C
T_i =	25.0	C
b =	0.7	
ΔH =	368200	Joule/kg of wood

Table 2

Relative Importance of Model Parameters for a Particle 2 cm in Diameter

Parameter	Sensitivity Range	Parameter Range Studied	Relative Importance
r_o	1.5 -- 3.0	0.5 - 2.0 cm	1
T_s	-38.1 -- -0.73	360 - 1050 C	2
k_c	-1.73 -- -0.46	0.1 - 0.4 Joule/M-Sec-K	3
ρ_w	1.0	615 - 2460 (Kg/M^3)	4
T_p	-0.66 -- -1.54	175 - 525 C	5
ΔH	0.5 -- 0.47	184100 - 763640 Joule/Kg	6
C_{pw}	0.28 -- 0.30	659 - 2636 Joule/Kg-K	7
k_w	-0.14 -- -0.07	0.1 - 0.4 Joule/M-Sec-K	8
C_{pg}	0.14 -- 0.13	600 - 2400 Joule/Kg-K	9
C_{pc}	0.07 -- 0.06	495.8 - 1983.2 Joule/Kg-K	10
b	-0.012 -- - 0.027	0.3 - 0.9	11
T_i	-0.0144 -- -0.015	0 - 300 C	12

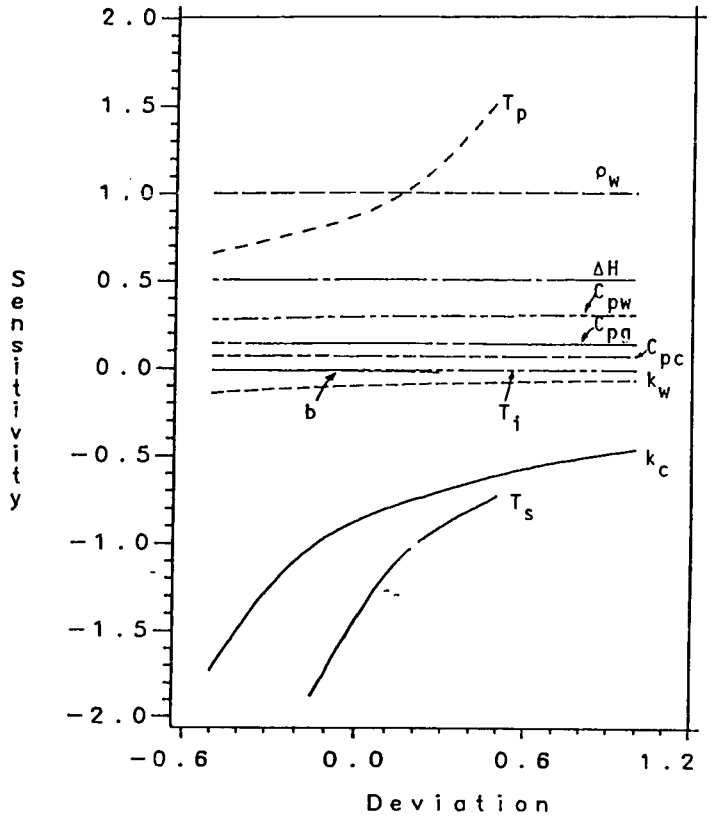

Figure 5 : Sensitivity of Model Parameters for a Particle of 2cm in Diameter

Particle Size and Density (r_o, ρ_w)

As expected, the pyrolysis time varied approximately quadratically with r (cylindrical geometry) and linearly with ρ_w indicating that for the size range studied, t_{pyr} is proportional to the mass of the sample.

Characteristic Temperatures (T_s, T_p, T_i)

For a particle 2 cm diameter, the imposed surface temperature has the greatest effect of all parameters in the determining pyrolysis time. When T_s is 525, 700, 875°C, the corresponding pyrolysis times are 8.8, 5.6, and 4.3 minutes. The pyrolysis temperature has a moderate influence on t_{pyr} when varied over a physically meaningful range. When T_p is varied from 263 to 350°C, t_{pyr} increases from 4.5 to 5.6 minutes. The initial temperature, T_i, has a negligible effect. The sensitivities of these parameters are illustrated in Figure 5. Plots of front position vs. time for a wide range of the parameters T_s, T_p, and T_i appear in Figures 6, 7, and 8.

Thermal Conductivities (k_c, k_w)

Due to the nature of the model, the thermal conductivity of the char is the most sensitive of all the physical properties considered. The thermal conductivity of the virgin solid however, has a negligible influence on the time required for complete pyrolysis. The comparison is best illustrated by the front position vs. time plots when the above parameters are varied (Figures 9, 10).

When k_c is varied from .1 to .4 J/msK t_{pyr} varies from 10 to 3 minutes. Over the same range of values for k_w, t_{pyr} varies from 6 to 5.2 minutes.

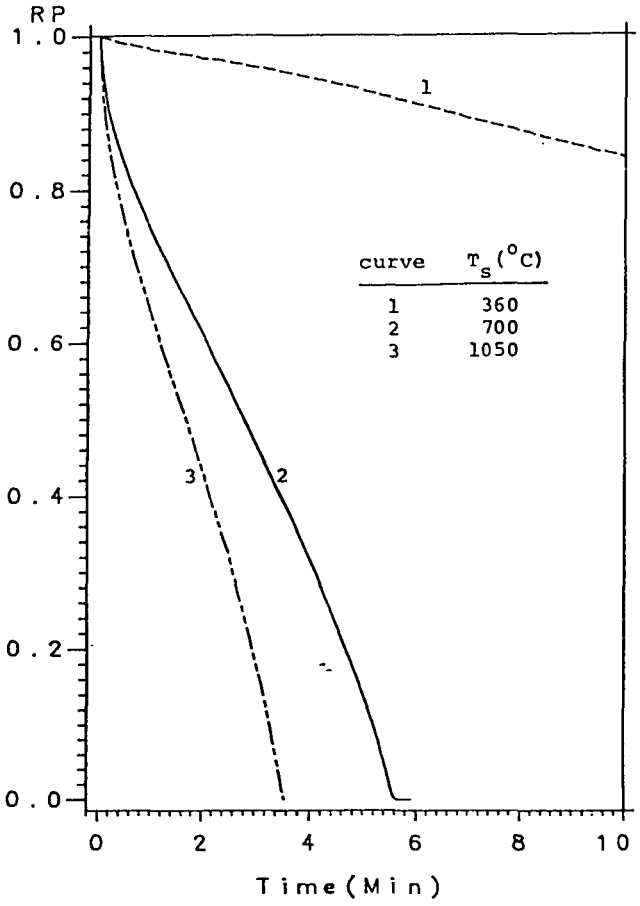

Figure 6: Pyrolyzing Front vs. Time curves at Three Surface Temperatures for a Particle of 2 cm Diameter

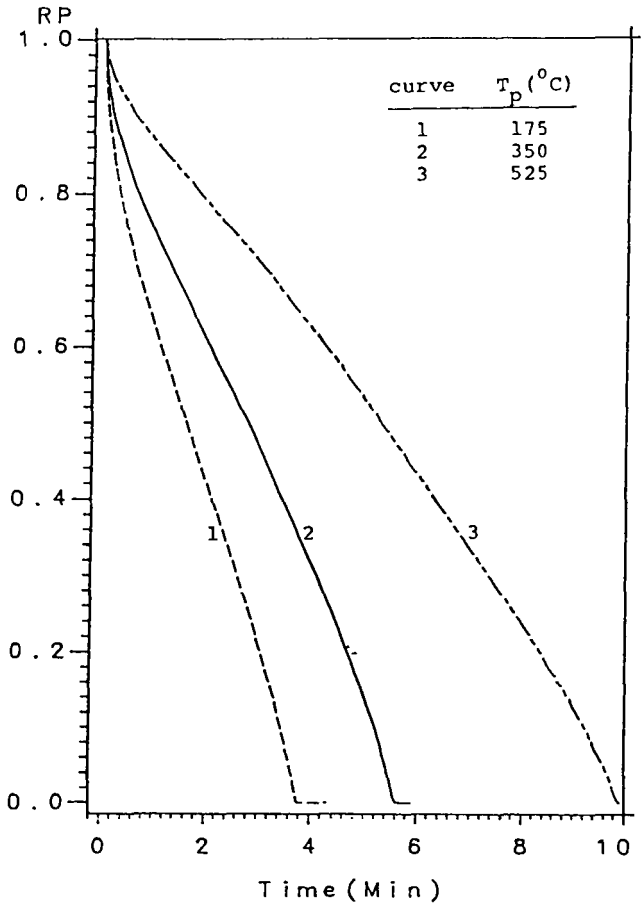

Figure 7 : Pyrolyzing Front vs. Time curves at Three Pyrolysis Temperatures for a Particle of 2 cm Diameter

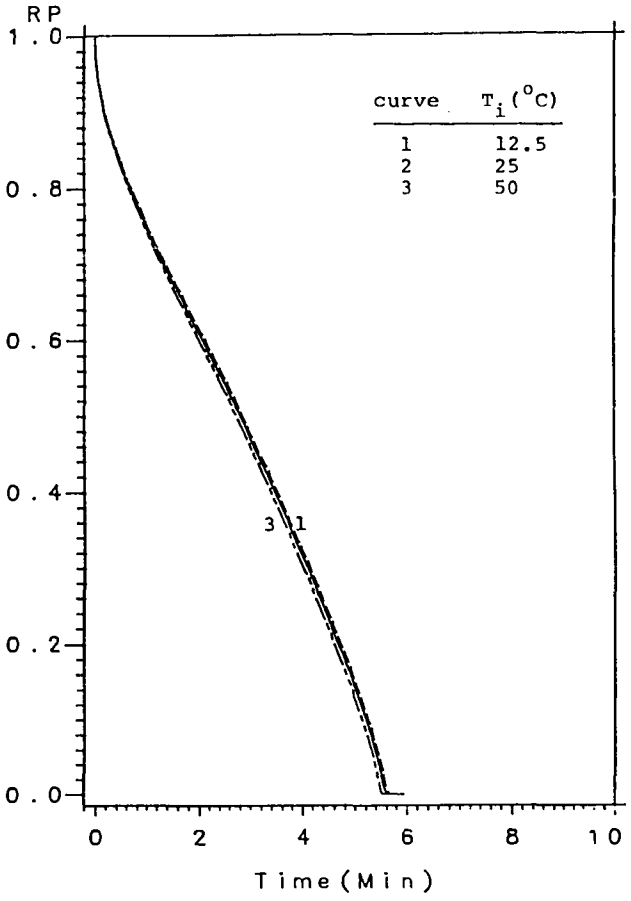

Figure 8: Pyrolyzing Front vs. Time Curves at Three Values of Initial Temperatures for a Particle of 1 cm Radius

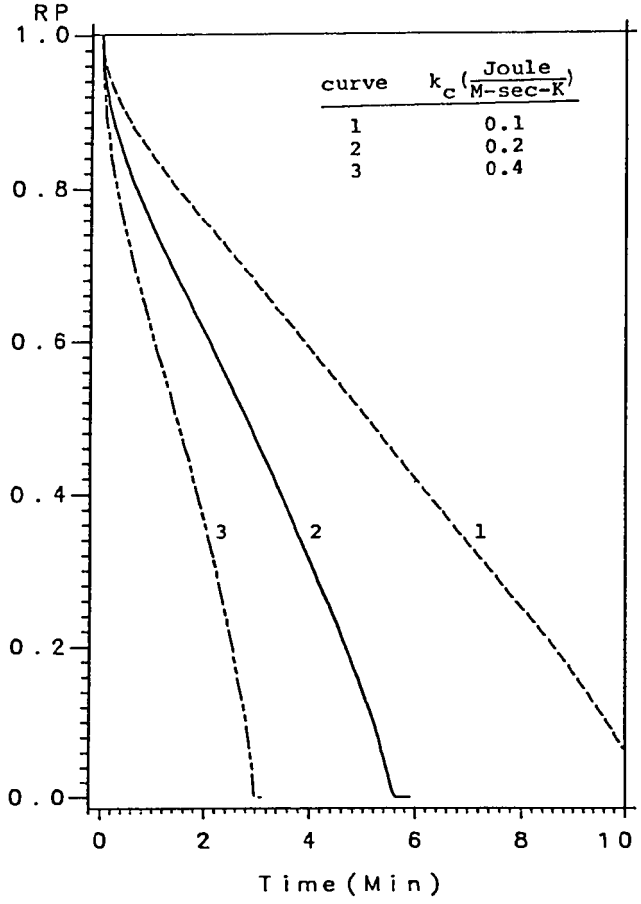

Figure 9 : Pyrolyzing Front vs. Time Curves at Three Values of Char Thermal Conductivity for a Particle of 1 cm Radius

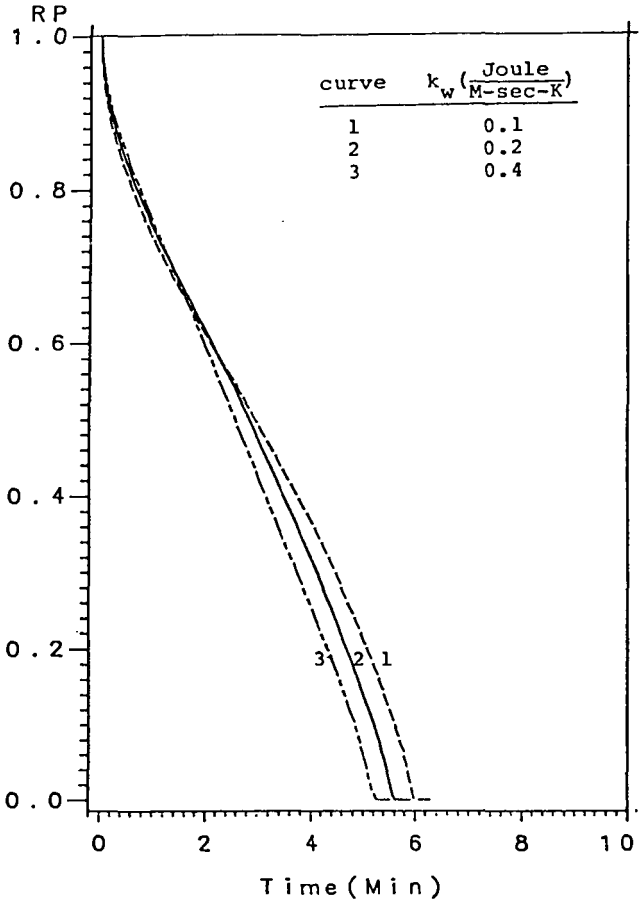

Figure 10: Pyrolyzing Front vs. Time Curves at Three Values of Thermal conductivity of Wood for a Particle of 1 cm Radius

Heat Capacities (C_{pc}, C_{pw})

The heat capacity of the unpyrolyzed solid, C_{pw}, has a greater influence on the rate of pyrolysis than the corresponding property for the resultant char, C_{pc}. The comparison is most directly illustrated in Figures 11 and 12.

Stoichiometric Coefficient (b)

When the stoichiometric coefficient of the gaseous product in the reaction

wood = b gas + c char

is varied over a wide range, there is virtually no change in the time required for pyrolysis (see Figure 13). It appears that the changing density of the char $\rho_c = \rho_w(1-b)$ counteracts the effect of the convective term in the energy balance.

Heat of Pyrolysis (H)

As illustrated in Figure 14, when the endothermic heat of primary pyrolysis varied from 184.1 to 736.4 J/g, the pyrolysis time increased from 4.2 to 8.4 minutes.

Summary

The results of any simulation using the phase-change model of pyrolysis are most significantly affected by the values of pyrolysis temperature, char thermal conductivity, and heat of pyrolysis.

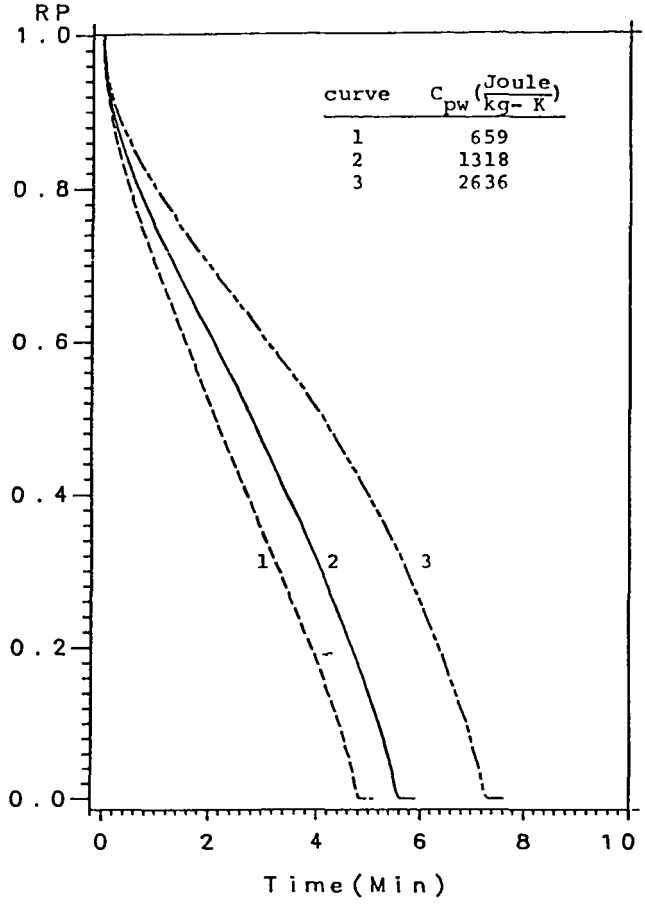

Figure 11: Pyrolyzing Front vs. Time Curves at Three Values of Heat Capacity of Wood for a Particle of 1 cm Radius

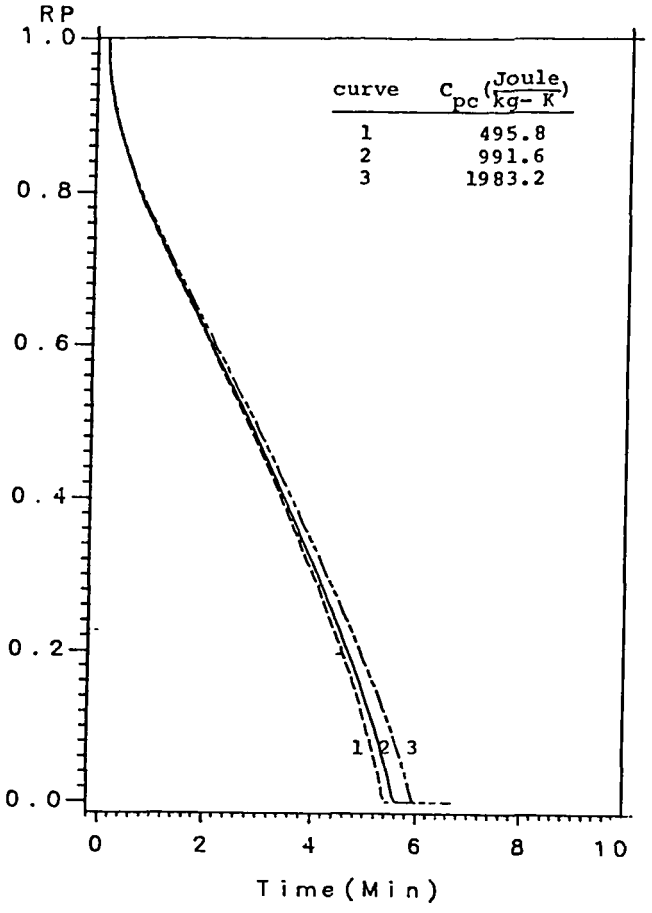

Figure 12: Pyrolyzing Front vs. Time Curves at Three Values of Heat Capacity of Char for a Particle of 1 cm Radius

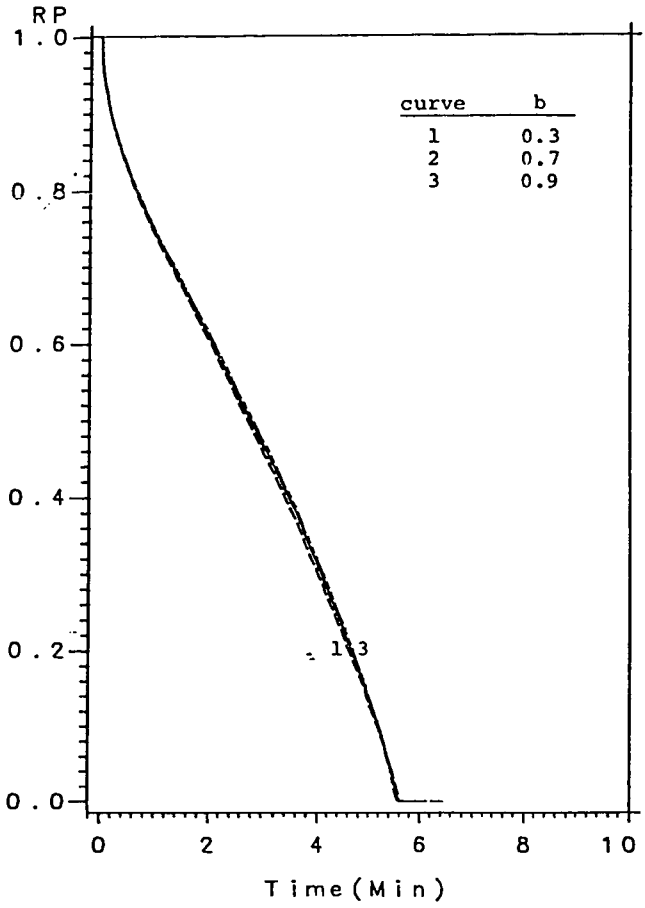

Figure 13: Pyrolyzing Front vs. Time Curves at Three Values of Stoichiometric Coefficient of Pyrolysis Gas for a Particle of 1 cm Radius

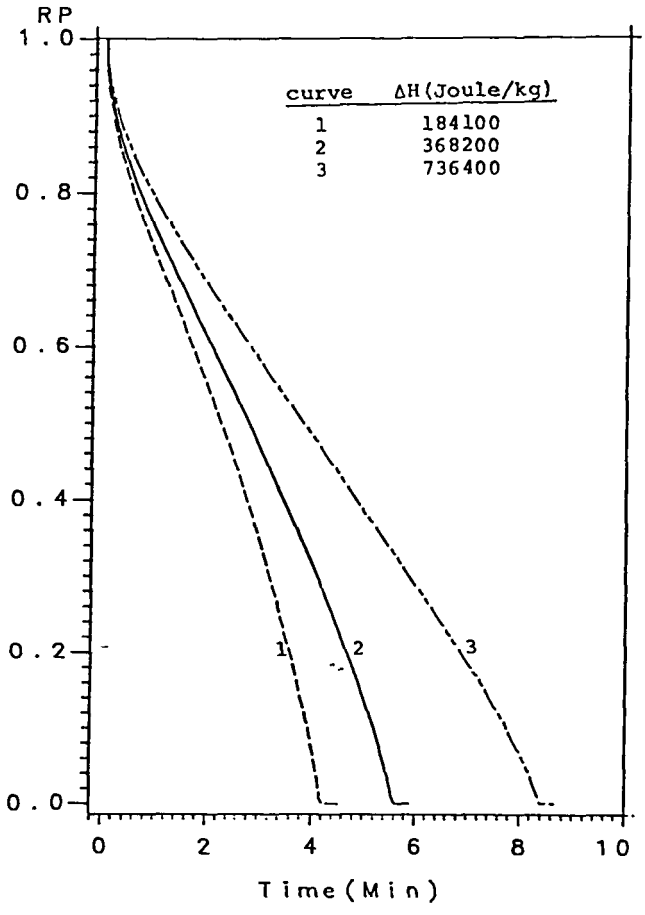

Figure 14: Pyrolyzing Front vs. Time Curves at Three Values of Heat of Pyrolysis for a Particle of 1 cm Radius

SINGLE PARTICLE SIMULATIONS

Up to the present time we have investigated only the case of a boundary condition of the first kind, in which the surface temperature is specified. The more useful case of a convective boundary condition (B.C. of 3rd kind) is currently under study. The choice to study the former problem was made on the basis of available experimental data. Investigators performing pyrolysis experiments on single particles usually measure and report surface temperature.

In one experiment (Kanury, 1966) a cylindrical specimen 1.75 cm in radius of pressed α-cellulose was placed in an externally-heated, rotating copper tube. Temperature profiles were recorded by thermocouples embedded at various radii. Measured surface and centerline temperatures are plotted in Figure 15. Using the parameters listed in Table 3 and the measured surface temperature as a boundary condition, the centerline temperature was calculated using the phase-change model. The calculated profile is also plotted in Figure 15.

The experimental profile displays plateaus at 120°C and 380°C corresponding to drying and pyrolysis temperatures. The calculated profile cannot reproduce the drying plateau because no phase change corresponding to drying was incorporated in the model. The plateau corresponding to pyrolysis however, was clearly observed. The measured surface temperature after complete pyrolysis was erratic because the thermocouple at the surface was not tightly bonded to the char.

In a second experiment (Roberts and Clough, 1963) the weight loss history of a 1 cm (radius) beech cylinder was recorded during pyrolysis in a nitrogen atmosphere. Using the parameters in Table 4 and the measured surface temperature, the weight vs. time curve was calculated. The results are shown in Figure 16. The heating rate of the oven used in the experiment was 20°C/min. Since the model predicts no weight loss until the surface temperature reaches the assumed

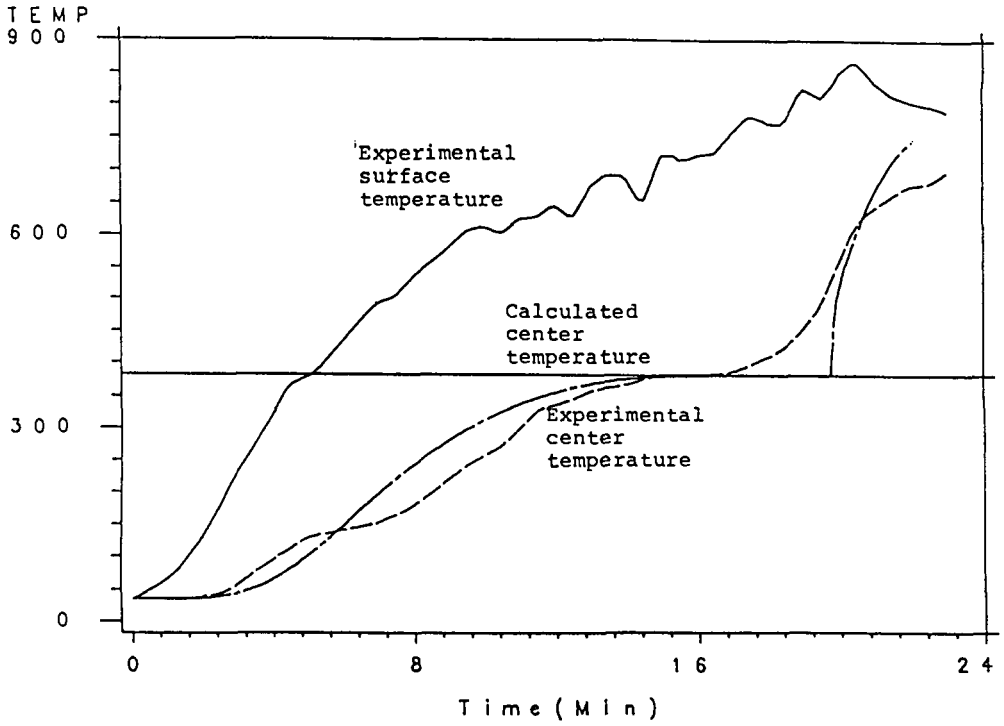

Figure 15 : Comparison between Experimental and Calculated Temperature History.

Table 3

Parameters and Properties Used to Simulate Kannry's Experiment

ρ_w	= 605	(Kg/M^3)
ρ_c	= (1-b) $_w$	(Kg/M^3)
k_w	= 0.14	(Joule/M-Sec-K)
k_c	= 0.06	(Joule/M-Sec-K)
C_{pc}	= 991.6	(Joule/Kg-K)
C_{pw}	= 1318.0	(Joule/Kg-K)
C_{pg}	= 1200	(Joule/Kg-K)
b	= 0.80	
H	= 100000	(Joule/Kg)
T_p	= 382	C
T_i	= 35	C

Table 4

Representative Values of Parameters and Properties Used in Model Calculation for Beech Cylinder

ρ_w	= 600.0	(Kg/M^3)
ρ_c	= (1-b) ρ_w	(Kg/M^3)
k_w	= 0.14	(Joule/M-Sec-K)
k_c	= 0.04	(Joule/M-Sec-K)
C_{pw}	= 1318.0	(Joule/M-Sec-K)
C_{pc}	= 991.6	(Joule/Kg-K)
C_{pg}	= 1200.0	(Joule/Kg-K)
b	= 0.61	
ΔH	= 100000	(Joule/Kg)
T_p	= 290	C
T_i	= 25	C

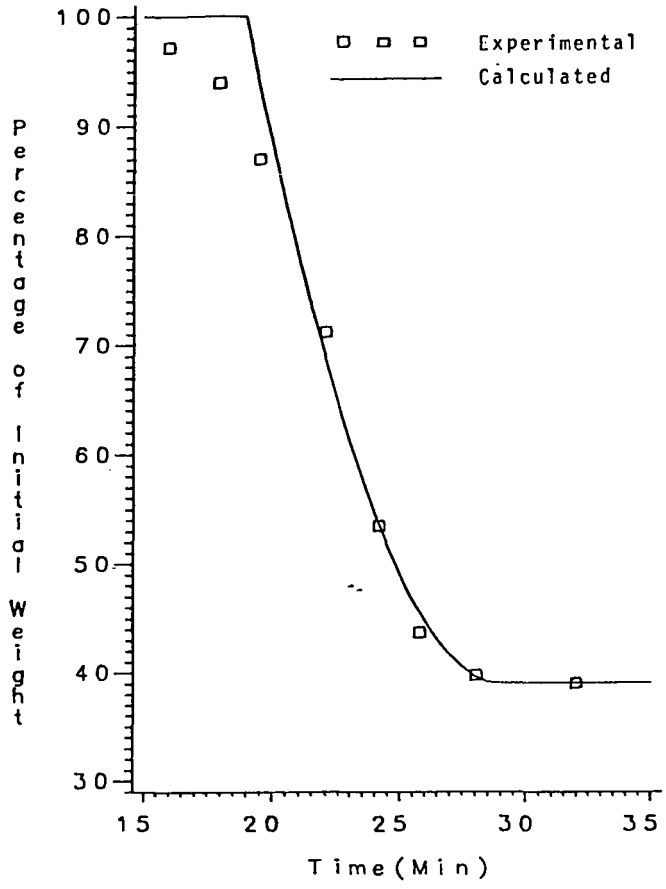

Figure 16: Comparison between Calculated and Experimental Weight/Time Curves for a Pyrolyzing Beech Cylinder.

pyrolysis temperature, it cannot reproduce that portion of the measured curve corresponding to low temperature pyrolysis.

PYROLYSIS ZONE OF A PACKED-BED GASIFIER

In order to simulate the pyrolysis zone of a packed-bed gasifier, the reactor was treated conceptually as two ideal reactors: one, a char combustor/gasifier and the second, a feed pyrolyzer. The gas temperature and flowrate exiting the gasification zone were used as input parameters for the pyrolysis simulation. The other boundary conditions were the offgas and feed temperatures.

The pyrolysis reaction is

$$\text{Feed} \longrightarrow \text{Char} + \text{Oil} + H_2O + \text{Gas}$$

The reaction is driven by the sensible heat in the char-derived gases from the combustion zone. The char-derived gas is considered inert and the offgas composition is obtained by simply mixing the char-derived gas flow with the volatile products of the pyrolysis reaction. The temperature of the gas, which is assumed to be the same as the surface temperature of the solid pellets, is used as the boundary condition of the kinetics-free model. We also assume that the pyrolysis portion of the reactor is characterized by plug flow, with no important radial gradients of mass or temperature.

Material balances were taken over the gas and solid phases.

$$dG_g/dZ = R_g \qquad dG_s/dZ = R_s$$

The energy balance was taken as

$$\frac{d}{dZ}(G_g C_{pg} T_g) = Q_s a + R_s \quad H_2$$

The generation terms are the flux ($Q_s a$) into the pellets and $R_s \Delta H_2$, the exothermic heat of reaction of the volatiles, both based on unit volume of reactor. ΔH_2 is the difference between the exothermic heat of the overall pryolysis reaction and the endothermic heat of the primary pyrolysis step used in the phase change model.

A Runge Kutta method was used to integrate the system of equations. An axial temperature profile for the bed was assumed. This profile was used in the phase change model to calculate the reaction rate and heat flux as a function of time. The velocity of the solid phase was constant (no particle shrinkage) so time was proportional to distance along the bed. The bed temperature was calculated and the process repeated until the boundary conditions were satisfied.

For the conditions listed in Table 5, the calculated profile illustrated in Figure 17 was obtained.

FUTURE WORK

A convective boundary condition (B.C. of 3rd kind) using effective heat transfer coefficients will be investigated. The heat transfer correlations for particles in packed beds will be modified to account for the escape of volatiles from the surface of the char. Single particle experiments are being planned in which the convective environment (gas temperature and velocity) of the sample will be controlled. Gas temperatures can be measured more easily than solid surface temperatures. In addition, packed-bed experiments with thermocouple-studded samples are planned.

Table 5

Operating Conditions for the Test Run on the Biomass Gasifier

Wood Pellett Feed Rate (Kg/Hour)	15.8
Air Feed Rate (Kg/Hour)	9.678
Steam Feed Rate (Kg/Hour)	1.941

Parameters of Char and Wood Pellets Used to Simulate the Test Run of the Biomass Gasifier

ρ_w	= 1230.0	Kg/M^3
ρ_c	$= \rho_w(1-b)$	Kg/M^3
C_{pw}	= 1318.0	Joule/Kg
C_{pc}	= 991.6	Joule/Kg
k_w	= 0.03	Joule/M-Sec-K
k_c	= 0.005	Joule/M-Sec-K
r_o	= 0.003175	m
T_p	= 300.0	C
T_i	= 25.0	C
b	= 0.8	
ΔH	= 62760	Joule/Kg of wood
ΔH_2	= -368200	Joule/Kg of wood

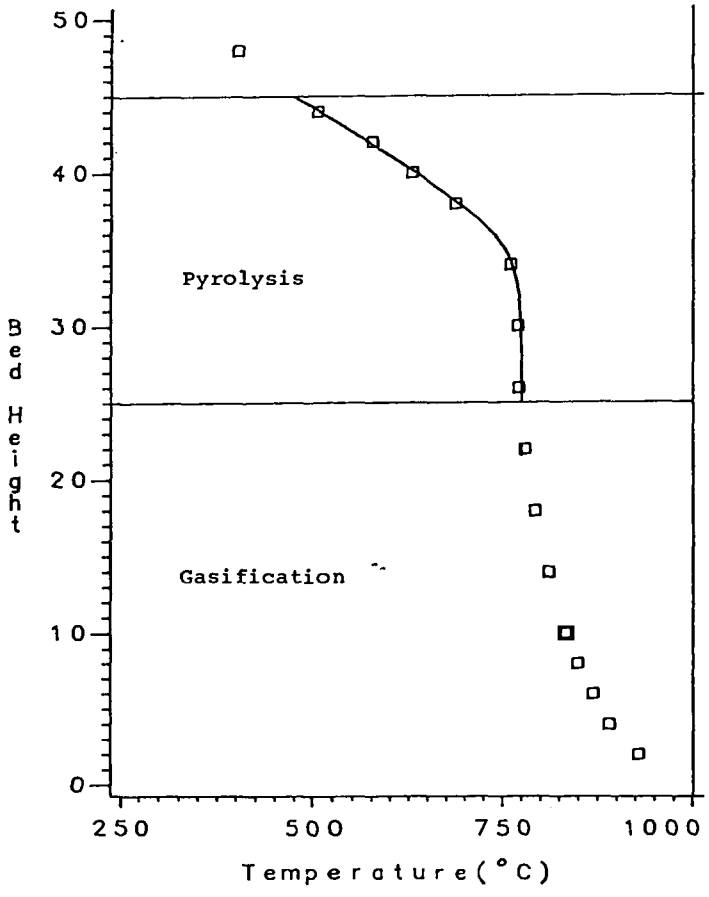

Figure 17: Comparison Between Calculated and Experimental Temperature Profiles in a Packed-Bed Gasifier.

Nomenclature

α	Thermal diffusivity
b	Stoichiometric coefficient of char in the pyrolysis reaction
B	Dimensionless parameter arising from the convective term in the char layer
c_p	Heat capacity
	Distance of pyrolyzing front from nearest grid point in the char layer
k	Thermal conductivity
M	Index of grid point in the char layer nearest the pyrolyzing front
N	Number of grid points
	Density
r	Radial position (r = 0 at center)
r_o	Cylinder radius at surface
R	Dimensionless radial distance (R = 0 at surface, R = 1 at center)
T	Temperature
	Dimensionless time
U,V	Dimensionless temperature
u_g	Velocity of exiting volatiles

Subscripts:

w	Wood layer, virgin solid
c	Char layer
p	Pyrolysis
s	Surface
g	Gas

References

Ackendon, J. R.; Hodgkins, W. R., Moving Boundary Problems in Heat Flow and Diffusion, Clarendon Press, Oxford (1975).

Bamford, C. H., Crank, J. and Malan, D. H., "The Combustion of Wood, Part I," Proc. of Cambridge Phil. Soc., 42, 166-184 (1946).

Carnahan, B., Luther, H. A., Wilkes, J. O., Applied Numerical Method, John Wiley and Sons, New York (1969).

Carslaw, H. S., Jaeger, J. C., Conduction of Heat in Solids, Oxford University Press, London (1959).

Fan, L. S., Fan, L. T., Tojo, K., Walawender, W. P., "Volume Reaction Model for Pyrolysis of a Single Solid Particle Accompanied by a Complex Reaction," Can. J. of Chem. Engr., 56, 603-609 (1978).

Maa, Sheng-Shyong P., "Influence of Particle Size and Environmental Condition on High Temperature Pyrolysis of the Cellulosic Material--I (Theoretical)," Combustion Science and Technology, 7, 257-269 (1973).

Muhlenkamp, S. P., "Pyrolysis of Living Wildland Fuels," Ph.D. Dissertation, University of Oklahoma, Norman, Oklahoma (1975).

Murty, K. A., Blackshear, P. L., "An X-Ray Photographic Study of the Reaction Kinetics of O-Cellulose Decomposition," Pyrodynamics, 4, 285-298 (1966).

Murty, K. A., "An Evaluation of The Physico-Chemical Factors Influencing the Burning Rate of Cellulosic Fuels and a Comprehensive Model for Solid Fuel Pyrolysis and Combustion," Ph.D. Dissertation, University of Minnesota (1969).

Roberts, A. F., Clough, G., "Thermal Decomposition of Wood in an Inert Atmosphere," Ninth Symposium (International) on Combustion, 158-166 (1963).

Roberts, D. L., "Numerical Solution of Heat Conduction Problem with a Change of Phase," Master Thesis, Texas Tech University (1981).

Stefan, Ann. Phys. u. Chem., N.F., 42, 269 (1891).

Wilson, D. G., Solomon, A. D., Boggs, P. T., Moving Boundary Problems, Academic Press (1978).